How MIMO capacity is linked with single element fading statistics

H. Özcelik* M. Herdin* R. Prestros* E. Bonek*

Abstract — **By analyzing comprehensive 8×8 MIMO measurements at 5.2 GHz in an indoor office environment, we demonstrate that MIMO capacity is mainly driven by the average receive SNR, since multipath richness does not vary a lot. We found that the channel matrix realizations measured at a single position are sufficient to predict capacity at all other positions in this specific environment. Deviations from this distinctive relation can be explained by correlation which is weakly linked to fading statistics. When the channel matrix coefficient magnitudes are Rice distributed, indicating dominant wave propagation leading to higher correlation, the capacity is typically lower than for strictly Rayleigh distributed channel matrix coefficient magnitudes (indicating rich multipath), *at a given SNR*.**

1 INTRODUCTION

Multiple-input multiple-output (MIMO) systems promise large information-theoretic capacities [1], enabling high data rate transmission, especially in rich multipath indoor scenarios. They offer spatial multiplexing gain by providing orthogonal spatial propagation paths. This gain is determined by the spatial structure of the MIMO channel. The channel capacity depends on the average receive SNR *and* the spatial multipath structure of the MIMO channel. This will be the topic of our paper.

The spatial multipath structure determines the complex correlation between all channel matrix elements and the fading statistics (i.e. the distribution of a single complex channel matrix element) directly. For given correlation, the fading statistics itself does not influence ergodic capacity significantly [2]. However, the fading statistics is not independent of the multipath structure. Low correlation, as it typically occurs in rich multipath scattering environments with large angular spread, induces large multiplexing gain leading to high capacity [3] [4].

This paper analyzes comprehensive measurements at 5.2 GHz in an indoor office environment with rich multipath. We will show that MIMO capacity is mainly driven by receive SNR, and explain deviations by inspecting fading statistics. Among others, this relates to the question what is more important for reaching high MIMO capacities, a high average receive SNR or rich multipath scattering [5] [4]. Additionally, we want to find out whether it is possible to give a rule of thumb for the channel capacity in indoor scenarios when the pathloss is given.

*Institut für Nachrichtentechnik und Hochfrequenztechnik, Technische Universität Wien, Gußhausstrasse 25/389, A-1040 Wien, Austria, e-mail: {hueseyin.oezcelik, markus.herdin, ralph.prestros, ernst.bonek}@tuwien.ac.at, tel.: +43 1 58801 38933, fax: +43 1 58801 38999.

2 MEASUREMENT

2.1 Measurement Setup

For the measurements, we used the wideband vector channel sounder RUSK ATM [6] with a measurement bandwidth of 120 MHz at a center frequency of 5.2 GHz. At the transmit side (Tx), a monopole antenna was mounted on a 2D positioning table where the position was controlled by the channel sounder by means of two stepping motors. The Tx antenna was moved to 20 possible x- and 10 possible y-positions on a rectangular grid with $\lambda/2$ spacing, forming a 20×10 virtual Tx matrix *without* mutual coupling. The receiver (Rx) was a directional 8-element uniform linear array (ULA) with 0.4λ inter-element spacing and two additional dummy elements. The antenna elements were printed dipoles with a backplane with 120° 3dB beamwidth; they were consecutively multiplexed to a single receiver chain.

For each Tx position the channel sounder measured 128 temporal snapshots of the frequency dependent transfer function between the Tx monopole and all Rx antennas. Within the measurement bandwidth of 120 MHz, 193 equidistant frequency samples of the channel coefficients were taken. Altogether, this resulted in a (128×193×8×200) 4-dimensional complex channel transfer matrix containing the channel coefficients for each temporal snapshot, frequency, Rx and Tx position. Since the measurement of the whole 4-dimensional channel transfer matrix took about 10 minutes, we measured at night to ensure stationarity.

2.2 Environment

The measurements were carried out in the offices of the *Institut für Nachrichtentechnik und Hochfrequenztechnik, Technische Universität Wien.* In to-

tal, 24 Rx positions were measured: one in a hallway - with line-of-sight (LOS) to Tx, 23 of them in several office rooms connected to this hallway - with non-line-of-sight (NLOS) to Tx , always with the (virtual) Tx array positioned in the same place in the hallway. Some rooms were amply, others sparsely furnished with wooden and metal furniture and plants. At each position, we rotated the Rx antenna to three different broadside directions D1, D2 and D3 (see Figure 1). These directions were angularly spaced by 120°. Thereby, we get 72 different 'scenarios', i.e. combinations of Rx positions and directions.

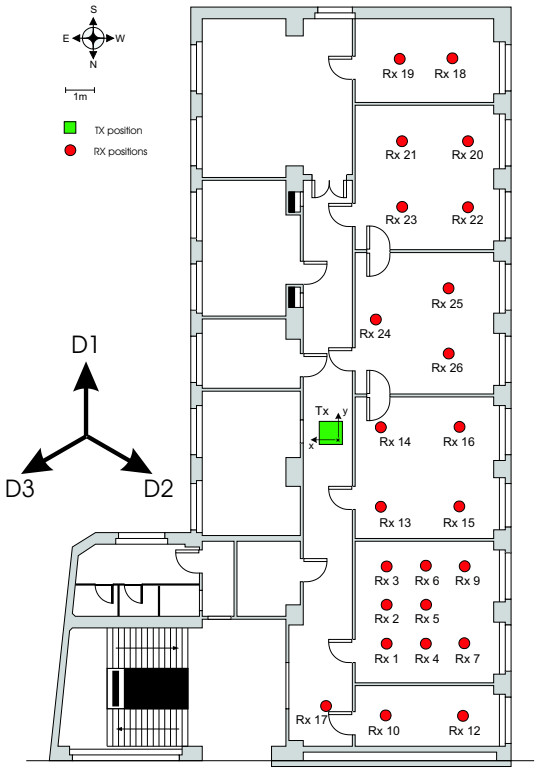

Figure 1: Map of measured indoor scenarios

3 DATA EVALUATION

3.1 Generating Different Channel Realizations

For further evaluations, we only used a 10×5 submatrix of the virtual 20×10 transmit matrix, in order to avoid large scale effects. Before we generated the MIMO channel realizations for each scenario, we averaged over all 128 temporal snapshots to increase the SNR leading to an 8×50 MIMO matrix for each frequency bin. The 50 Tx positions were used to create different spatial realizations of an 8×8 MIMO channel matrix. We grouped 8 adjacent Tx positions in x-direction together to form a virtual 8-element ULA and moved this virtual Tx array over the 10×5 Tx matrix. This resulted in $3 \cdot 5 = 15$ spatial realizations of an 8×8 MIMO channel matrix. We also used the 193 different frequency bins as realizations giving us a total of $15 \cdot 193 = 2.895$ different realizations of the MIMO channel matrix for each scenario.

3.2 Capacity, Normalization

Considering a channel unknown at Tx, the ergodic MIMO capacity for each spatial and frequency realization was calculated by [1]

$$C = \log_2 \det(\mathbf{I}_m + \frac{\rho}{n}\mathbf{H}\mathbf{H}^H) \qquad (1)$$

where $\mathbf{I}_m$ denotes the $m \times m$ unity matrix, ρ the mean receive SNR, n the number of Tx antennas and $\mathbf{H}$ the normalized $m \times n$ MIMO channel matrix. Here, $m = n = 8$.

Since the measured MIMO matrices include the pathloss, we had to normalize them properly. We distinguish two different cases: the capacity *with* and *without* pathloss considered. In the first case we divided all measured MIMO matrices by a constant normalization factor. This normalization factor was chosen such that the equivalent single-input single-output (SISO) pathloss

$$PL_{SISO} = \frac{1}{m \cdot n} \sum_{i=1}^{m} \sum_{j=1}^{n} |h_{ij}|^2 \qquad (2)$$

for a single measurement (reference) scenario was equal to 0 dB on average over all spatial and frequency realizations. Here, h_{ij} denote the channel matrix elements of the corresponding normalized channel matrix $\mathbf{H}$. As reference scenario we chose position Rx26, direction D3 (Rx26D3).

By setting ρ to 20 dB, we get therefore an average receive SNR of 20 dB for this reference scenario, but due to different pathloss values different values of the average receive SNR for all other scenarios. This corresponds to a system with fixed transmit power where the capacity is given by both the multipath richness and the average receive SNR.

In the second case we used different normalization factors for each measurement scenario, such that the average receive SNR was equal to 20 dB for each scenario, i.e. we normalized the pathloss out. This would correspond to a MIMO system with transmit power control, i.e. the average receive SNR is fixed and only the multipath richness determines the capacity.

For the following evaluations, we always consider the average MIMO capacity by averaging over all spatial and frequency realizations for each scenario.

4 RESULTS

First, we calculated the average MIMO capacity with pathloss considered. Figure 2 shows the scatter plot of average 8×8 MIMO capacity vs. SISO pathloss of the measured channel matrices. Each point in this plot corresponds to one scenario. Additionally, the capacity resulting from the MIMO channel realizations at Rx26D3, when varying the receive SNR (and therefore artificially varying the SISO pathloss!) is shown as a solid line.

As can be seen, the average capacity has a clear downward trend with increasing pathloss. Apart from some exceptional scenarios, the MIMO capacity values are well approximated by this solid line. This means that the capacity is mainly determined by the average receive SNR, or equivalently, for a constant transmit power, by the SISO pathloss of the respective Rx position/direction. Evidently, multipath richness does not vary a lot.

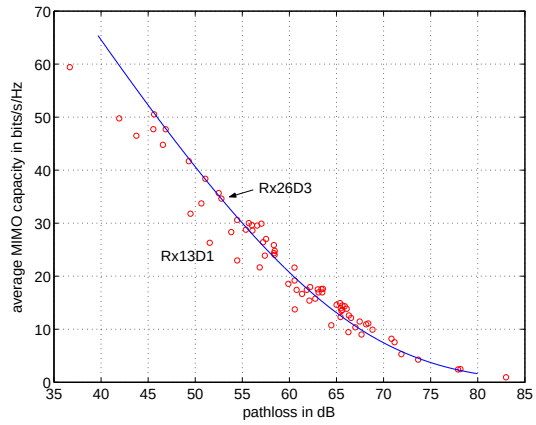

Figure 2: Scatter plot of average 8×8 MIMO capacity vs. pathloss for 20 dB receive SNR at Rx26D3

The underlying reason for the deviation of some capacities from the solid line can be investigated by having a closer look at the fading statistics.

Let's first consider the reference position Rx26D3: Figure 3 shows the probability density functions (pdf) of the magnitudes, i.e. the fading statistics, of the measured channel matrix coefficients (solid line) and a Rayleigh distribution (dashed line) with *same mean power* as the measured channel. The fading statistics of this position is Rayleigh, indicating rich multipath scattering without dominant multipath components.

In contrast, if we take a look at scenario Rx13D1 (Fig. 4), we see that the fading statistics deviates strongly from Rayleigh. Assuming Rice fading in this scenario we estimated a Ricean K-factor of 3.6 using the method described in [7]. The dash-dotted

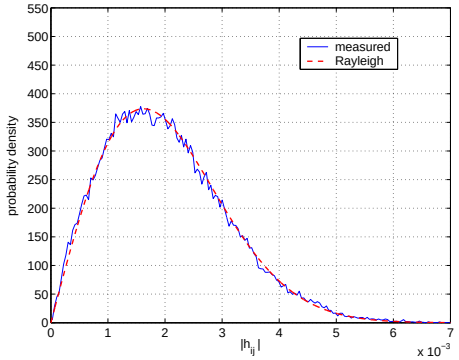

Figure 3: Fading statistics at Rx26D3

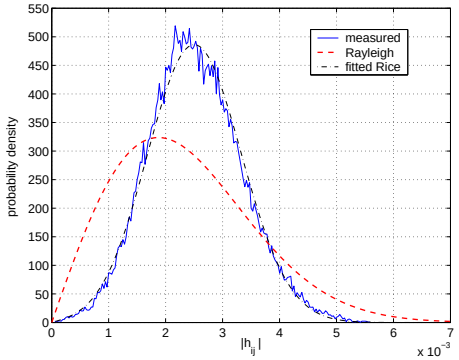

Figure 4: Fading statistics at Rx13D1

line shows the resulting Rice distribution, which is a good approximation to the measured pdf. In the majority of the scenarios, the distribution of the measured channel matrix coefficients can be well described by either Rayleigh or Rice distributions.

In order to focus on the effect of the multipath structure on capacity, we consider MIMO capacity *without* pathloss (see section 3.2) in the following. In Figure 5, the 8×8 MIMO capacity vs the Rice factor for each scenario is shown, now with pathloss normalized out. The capacity variations in this plot are only due to differences in the multipath structure. Assuming that the second order statistics are a complete description of the underlying radio channel, this is equivalent to different correlation.

There is a clear trend of decreasing capacity with increasing Ricean K-factor. Higher K-factor means dominant multipath components leading to higher correlation and therefore lower capacity. However, even in scenarios with Rayleigh fading (Ricean K-factor of 0) there is a large capacity variation. The reason for this is that Rayleigh fading can occur with both low and high correlation, as long as

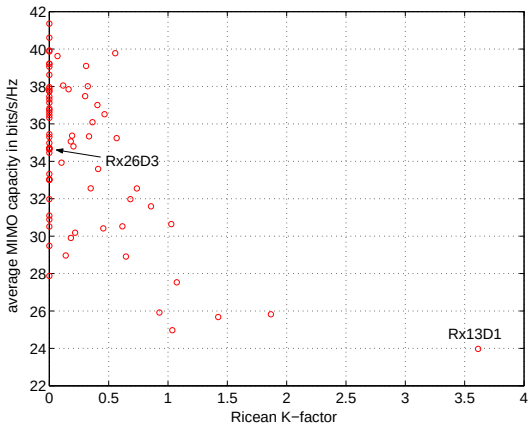

Figure 5: Scatter plot of average (normalized) MIMO capacity vs. Ricean K-factor for 20 dB receive SNR for each measurement scenario

there are enough independent multipath components. Rich multipath scattering with a large angular spread induces Rayleigh fading with *low correlation* resulting in high capacity, whereas a small angular spread induces Rayleigh fading with *high correlation* leading to low capacity.

Generally, we can say that high correlation resulting in low capacity is more likely to appear in scenarios with dominant multipath components inducing Rice fading.

5 CONCLUSIONS

Analyzing comprehensive measurement carried out in an indoor office environment at 5.2 GHz, we found that the MIMO capacity is mainly determined by the average receive SNR since multipath richness does not vary a lot.

Having found channel matrix realizations at *one* position, we can predict capacity at all other positions in this environment. Meaningfully exploited, this finding can save quite some effort in measuring MIMO systems. Deviations from this distinctive relationship can be explained by different correlation, linked weakly to the fading statistics.

Although fading statistics itself (i.e. for given correlation) does not influence the capacity a lot, we find that higher Rice factors are linked to lower capacity. The Rice distribution indicates dominant wave propagation causing high correlation (low angular spread) and therefore lower capacity. Of course, for a given Ricean K-factor, the correlation can vary.

6 Acknowledgments

We would like to thank Helmut Hofstetter (ftw) for help with the measurements, Werner Weichselberger for fruitful comments and T-Systems Nova GmbH for providing an eight element uniform linear array of printed dipoles.

References

[1] G.J. Foschini and M.J. Gans, "On limits of wireless communications in a fading environment when using multiple antennas," *Wireless Personal Communications*, vol. 6, no. 3, pp. 311–335, March 1998.

[2] C.G. Günther, "Comment on 'estimate of channel capacity in Rayleigh fading environment'," *IEEE Transactions on Vehicular Technology*, vol. 45, pp. 401–403, May 1996.

[3] D.S. Shui, G.J. Foschini, M.J. Gans, and J.M. Kahn, "Fading correlation and its effect on the capacity of multielement antenna systems," *IEEE Transactions on Communications*, vol. 48, no. 3, pp. 502–513, March 2000.

[4] H. Özcelik, M. Herdin, H. Hofstetter, and E. Bonek, "A comparision of measured 8×8 MIMO systems with a popular stochastic channel model at 5.2 GHz," *ICT*, vol. 2, pp. 1542–1546, 2003.

[5] D.P. McNamara, M.A. Beach, P.N. Fletcher, and P. Karlsson, "Capacity variation of indoor multiple-input multiple-output channels," *Electronics Letters*, vol. 36, no. 24, pp. 2037–2038, November 2000.

[6] R.S. Thomä, D. Hampicke, A. Richter, G. Sommerkorn, A. Schneider, U. Trautwein, and W. Wirnitzer, "Identification of time-variant directional mobile radio channels," *IEEE Transactions on Instrumentation and Measurement*, vol. 49, pp. 357–364, April 2000.

[7] L.J. Greenstein, D.G. Michelson, and V. Erceg, "Moment-method estimation of the Rician K-factor," *IEEE Communications Letters*, vol. 3, pp. 175–176, June 1999.